Computational Methods for Differential Equations
http://cmde.tabrizu.ac.ir
Vol. 6, No. 1, 2018, pp. 53-62

Numerical treatment for nonlinear steady flow of a third grade fluid in a porous half space by neural networks optimized

Mohsen Alipour*
Department of Mathematics, Babol Noshirvani University of Technology,
Shariati Ave., Post Code: 47148-71167, Babol, Iran.
E-mail: m.alipou2323@gmail.com; m.alipour@nit.ac.ir

Kobra Karimi
Department of Mathematics, Buin Zahra Technical University,
P.O. Box 34517-45346, Buin Zahra, Qazvin, Iran.
E-mail: kobra.karimi@yahoo.com

Abstract In this paper, steady flow of a third-grade fluid in a porous half space has been considered. This problem is a nonlinear two-point boundary value problem (BVP) on semi-infinite interval. The solution for this problem is given by a numerical method based on the feed-forward artificial neural network model using radial basis activation functions trained with an interior point method. Moreover, to confirm the performance of the proposed technique, our results are compared with other available results. Numerical results demonstrate the validity and applicability of the technique.

Keywords. Feed forward neural network, Radial basis functions, Semi infinite, Steady flow, Third-grade fluid.

2010 Mathematics Subject Classification. 35A35, 65Mxx, 34K28, 92B20.

1. Introduction

Recently, the non-Newtonian fluids have been studied in industrial and natural problems. The governing equations of non- Newtonian fluids are of higher order than the Navier-Stokes equations. The fluids of the differential type have received special attention among the many models which have been used to describe the non-Newtonian behaviour demonstrated by certain fluids. Among the several non-Newtonian fluid models, much attention has been paid to the simplest subclass of viscoelastic fluids known as the second grade. The modelling of polymeric flow in porous space has essential focus on the numerical simulation of viscoelastic flows in a specific pore geometry model, for example, capillary tubes, undulating tubes, packs of spheres or cylinders [12, 13, 20]. The third-grade fluid model represents a further, although inconclusive, attempt towards a more comprehensive description of the behaviour of viscoelastic fluids. Also, the flows of such fluids in porous medium are quite prevalent in many engineering fields such as enhanced oil recovery, paper and

Received: 11 May 2017 ; Accepted: 2 December 2017.
* Corresponding author.

textile coating, and composite manufacturing processes. Recently, many interesting problems dealing with the flows of non-Newtonian fluids are made by Rajagopal and Na [17, 16] and abbasbandy et al.[1, 4, 3, 5, 2, 18].

2. Problem Statement

In [1], Hayat et al, have discussed the flow of a third-grade fluid in a porous half space. For unidirectional flow, the authors in [20] have generalized the relation

$$(\bigtriangledown p)_x = -\frac{\mu\varphi}{k}(1+\frac{\alpha}{\mu}\frac{\partial}{\partial t})u, \tag{2.1}$$

for a second grade fluid to the following modified Darcy's Law for a third grade fluid,

$$(\bigtriangledown p)_x = -[\mu+\alpha\frac{\partial}{\partial t}+2\beta(\frac{\partial}{\partial y})^2]\frac{\varphi u}{k}. \tag{2.2}$$

In the above equations u, μ and p, respectively, denote the fluid velocity, dynamic viscosity and the pressure. α, β are material constants and k and φ, respectively represent the permeability and porosity of the porous half space which occupies the region $y > 0$. In [12], Hayat et al. have defined a non dimensional fluid velocity f and the coordinate z

$$z = \frac{V_0}{\nu}y,\ f(z) = \frac{u}{V_0}, \tag{2.3}$$

where $V_0 = u(0,t)$ and $\nu = \frac{\mu}{\rho}(\rho is the fluid density)$ represents the kinematic viscosity. The boundary value problem modelling the steady state flow of a third grade fluid in a porous half space becomes (see for more details [12, 6])

$$\frac{d^2f}{dz^2}+b_1(\frac{df}{dz})^2\frac{d^2f}{dz^2}-b_2f(\frac{df}{dz})^2-b_3f=0, \tag{2.4}$$

$$f(0)=1,\ f(z)\to 0\ as\ z\to\infty. \tag{2.5}$$

Above parameters are as follows:

$$b_1 = \frac{6\beta V_0^4}{\mu\nu^2}, \tag{2.6}$$

$$b_2 = \frac{2\beta\varphi V_0^2}{k\mu}, \tag{2.7}$$

$$b_3 = \frac{\varphi\nu^2}{kV_0^2}. \tag{2.8}$$

It is clear the parameters are not independent, since

$$b_2 = \frac{b_1b_3}{3}. \tag{2.9}$$

TABLE 1. Some well-known functions that generate globally supported RBFs.

Name of functions	Definition
Thin plate (polyharmonic) splines (TPS)	$(-1)^{k+1}r^{2k}\log(r)$
Gaussian (GA)	$\exp(-cr^2)$
Inverse multiquadrics (IMQ)	$1/\sqrt{r^2+c^2}$
Multiquadrics (MQ)	$\sqrt{1+(cr)^2}$
Conical splines	r^{2k+1}
Exponential spline	$\exp(-cr)$

3. Radial Basis Functions

Let $R^+ = \{x \in R, x \geq 0\}$ be the non-negative half-line and let $\phi : R^+ \to R$ be a continuous function with $\phi(0) \geq 0$. A radial basis functions (RBFs) on R^d is a function as follows

$$\phi(\|X - X_i\|), \tag{3.1}$$

where $X, X_i \in R^d$, and $\| \,.\, \|$ denotes the Euclidean distance between X and X_i. If one chooses N points $\{X_i\}_{i=1}^N$ in R^d then

$$s(X) = \sum_{i=1}^{N} \lambda_i \phi(\| X - X_i \|), \ \lambda_i \in R, \tag{3.2}$$

is called a radial basis function as well [9]. In Table 1 some commonly used globally supported RBFs are listed. In the radial basis functions $r = \|.\|_2$ denotes the Euclidean distance and c is a positive constant which is called a shape parameter. This constant prescribes the flatness of the radial basis function and specially has an important role to improve the stability and accuracy of the computational techniques based on the radial basis functions.

$$s(X) = \sum_{i=1}^{N} \lambda_i \phi(\| X - X_i \|), \ \lambda_i \in R, \tag{3.3}$$

The radial basis functions are very efficient tools for interpolating scattered data in multidimensional complex domain ([15, 11, 21, 19]). For a given set of scattered nodes $\{\mathbf{x}_i\}_{i=1}^N \in R^d$ and a real valued set $f(\mathbf{x}_i)$, $i = 1, \ldots, N$, a radial basis function interpolant, $\tilde{f}$, is a linear combination of radial basis functions centered at the discrete nodes $\mathbf{x}_j$ as follow:

$$\tilde{f}(\mathbf{x}) = \sum_{j=1}^{N} \alpha_j \phi(r_j) + \sum_{k=1}^{m} \lambda_k p_k(\mathbf{x}), \tag{3.4}$$

where $r_j = \|\mathbf{x} - \mathbf{x}_j\|_2$ is the Euclidean distance and $\{p_1(\mathbf{x}), p_2(\mathbf{x}), \ldots, p_m(\mathbf{x})\}$ is a set of monomial functions which is a basis for the space of polynomials up to degree s in R^d, π_s^d, moreover, m and s are related as $m = \begin{pmatrix} s+d \\ d \end{pmatrix}$. Also $\{\alpha_j\}_{j=1}^N \cup \{\lambda_k\}_{k=1}^m$

are unknown coefficients which can be estimated for any sets of interpolation points $\{\xi_i\}_{i=1}^N$ by satisfying the interpolation equations

$$f(\xi_i) = \tilde{f}(\xi_i) = \sum_{j=1}^{N} \alpha_j \phi(\|\xi_i - \mathbf{x}_j\|_2) + \sum_{k=1}^{m} \lambda_k p_k(\xi_i), \quad i = 1, \ldots, N, \tag{3.5}$$

and also the following additional orthogonality conditions:

$$\sum_{j=1}^{N} \alpha_j p_k(\xi_i) = 0, \quad k = 1, \ldots, m. \tag{3.6}$$

For simplicity the above equations can be presented in the following matrix form,

$$\begin{pmatrix} \Phi & P \\ P^T & 0 \end{pmatrix} \begin{pmatrix} \alpha \\ \lambda \end{pmatrix} = \begin{pmatrix} F \\ 0 \end{pmatrix},$$

where Φ is a $N \times N$ matrix with $\Phi_{i,j} = \phi(\|\xi_i - \mathbf{x}_j\|_2), \quad i, j = 1, \ldots, N$, which is clearly a symmetric and dense matrix for globally supported RBFs, P is a $N \times m$ matrix, with $P_{i,j} = p_j(\xi_i)$, and $F_i = f(\xi_i)$. In this article, the Gaussian basis is applied.

4. Neural network modeling

Neural networks have been successfully applied to a variety of real world classification tasks in industry, business, and sciences [8], and also artificial neural networks are used extensively as universal function approximators. The solution $f(x)$ of the differential equation along with its n^{th} order derivative $f^{(n)}$ can be approximated by the following continuous mapping in neural network [14].

$$\hat{f}(\eta) = \sum_{i=1}^{m} \delta_i g(w_i \eta + \beta_i), \tag{4.1}$$

$$\hat{f}^{(n)}(\eta) = \sum_{i=1}^{m} \delta_i \frac{d^n}{d\eta^n} g(w_i \eta + \beta_i), \tag{4.2}$$

where m is the number of neurons, g is called the activation function, δ, w, and β are real-valued bounded adaptive parameters or weights, written as:

$$W = (\delta_1, \delta_2, ..., \delta_m, w_1, w_2, ..., w_m, \beta_1, \beta_2, ..., \beta_m). \tag{4.3}$$

In this paper we consider radial basis g_{RB} as an activation function.

$$g_{RB} = e^{-t^2}, \tag{4.4}$$

Differential equation neural networks using radial basis have been developed to approximate solutions of the Eq. (4), by following mapping we approximate $f(\eta)$, $f^{'}(\eta)$ and $f^{''}(\eta)$ as:

$$\hat{f}(\eta) = \sum_{i=1}^{m} \delta_i e^{-(w_i \eta + \beta_i)^2}, \tag{4.5}$$

$$\hat{f}'(\eta) = \sum_{i=1}^{m} -2\delta_i w_i (w_i\eta + \beta_i) e^{-(w_i\eta+\beta_i)^2}, \tag{4.6}$$

$$\hat{f}''(\eta) = \sum_{i=1}^{m} -2(\delta_i (w_i^2 e^{-(w_i\eta+\beta_i)^2} - 2(w_i\eta + \beta_i)^2 w_i^2 e^{-(w_i\eta+\beta_i)^2})). \tag{4.7}$$

In our implementation, the following shifted Chebyshev-Gauss-Lobato points, $\{\varsigma_r\}_{r=0}^{K}$ are used as the collocation nodes:

$$\varsigma_r = \frac{Lx_r + L}{2(1 - x_r)}, \quad r = 0, \ldots, K, \tag{4.8}$$

where $\{x_r\}_{r=0}^{K}$ are standard Chebyshev-Gauss-Lobato points,

$$x_r = -\cos(\frac{2r\pi}{2K+1}), \quad r = 0, \ldots, K.$$

The fitness function ε has been developed for the transformed equation (4) using neural network models by defining the unspecified error as the sum of mean squared errors:

$$\varepsilon = \varepsilon_1 + \varepsilon_2. \tag{4.9}$$

The error term ε_1 is associated with the differential equation and given as

$$\varepsilon_1 = \frac{1}{K-1} \sum_{k=1}^{K-1} (\hat{f}''_k + b_1(\hat{f}')^2 \hat{f}''_k - b_2 \hat{f}(\hat{f}')^2 - b_3 \hat{f}). \tag{4.10}$$

Similarly, the error term ε_2 is for initial and boundary conditions, and is given as

$$\varepsilon_2 = \frac{1}{2}((\hat{f}_{\varsigma_0} - 1)^2 + (\hat{f}_{\varsigma_K})^2). \tag{4.11}$$

It is clear that for weights δ, w, and β for which the error functions ε_1 and ε_2 approach zero, the value of fitness ε also approaches zero, thus the proposed solution $\hat{f}$ given in Eq. (15), approaches the exact solution f. The neural network diagram for model 2.4 is shown in Figure 1. Learning methodology based on the interior point method (IPM) is used for training weights of the three neural networks for the nonlinear steady flow of a third grade fluid in a porous half space [23, 10, 22].

5. Numerical Results and discussion

In this section, the proposed numerical technique is used to investigate the behaviour of a third grade steady fluid flow in a porous half space. In Table 2, the computed results for non-dimensional parameter $f^{'}(0)$ are reported. Moreover, to confirm the performance of the proposed technique, our results are compared with other available results. The results are obtained by setting $n = 10$ and $L = 5$. The presented results in Table 2 show a good agreement between our approximate solutions and other numerical results. In Figure 2, the effect of the model parameter b_1 on the profile of $f(x)$, for the fixed value $b_3 = 1.5$ is illustrated. The results show that increasing or decreasing the value of b_2 has no sensible effects on profiles of $f(x)$.

FIGURE 1. Neural network diagram for model 2.4.

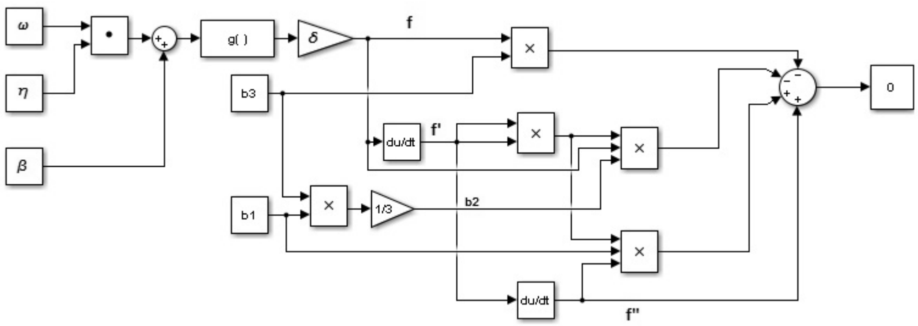

TABLE 2. Approximate results for $f^{'}(0)$ for various values of b_1 and b_3, ($b_2 = \frac{b_1 b_3}{3}$).

b_1	b_3	*present method*	*Shooting method* ([7])	*Rational Legendre Tau method* ([7])
0.3	0.5	−.691280234	−0.691280	−0.691493
0.6		−.678305971	−0.678301	−0.678511
0.9		−.667395223	−0.667327	−0.667528
0.6	0.3	−.533309395	−0.533303	−0.533545
	0.6	−.738005808	−0.738008	−0.738116
	0.9	−.887468383	−0.887467	−0.887350
	1.2	−1.00865312	−1.008653	−1.008516

Moreover, the effect of b_3 on the profile of $f(x)$, for the fixed value $b_1 = 0.5$ is demonstrated in Figure 3. Regarding Figure 3, it is evident that for the fixed value of b_1, the profiles of $f(x)$ decrease by increasing the values of b_3. In addition, to illustrate the accuracy and performance of the method in Figure 4, absolute values of the residual functions for some cases of the model parameters have been plotted. The results confirm the efficiency and accuracy of the method.

FIGURE 2. Profiles of $f(x)$ for various values of b_1 and $b_3 = 1.5$.

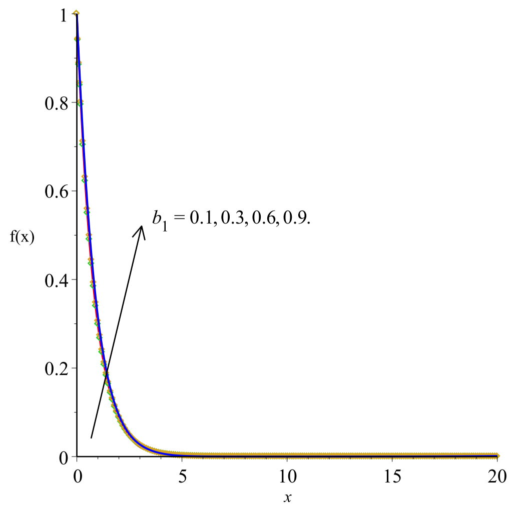

FIGURE 3. Profiles of $f(x)$ for various values of b_3 and $b_1 = 0.5$.

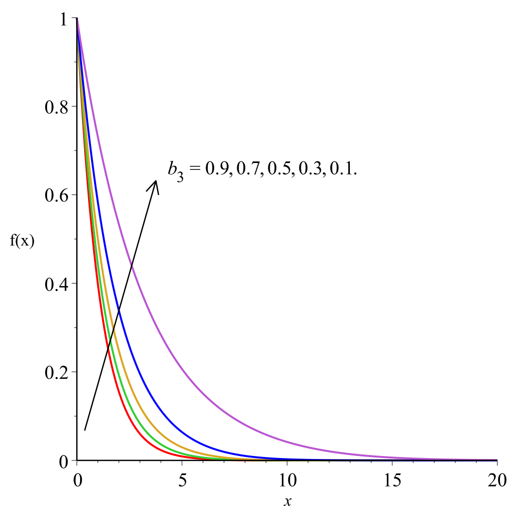

6. Conclusions

In this paper, we had proposed an approach for numerical solving the nonlinear steady flow of a third grade fluid in a porous half space based on neural network. The results achieved, had been compared with other avaliable results. These results show that the neural network works very well. The parallel processing property of

FIGURE 4. Graphs of the $|Res(\eta)|$ for four cases of the model parameters.

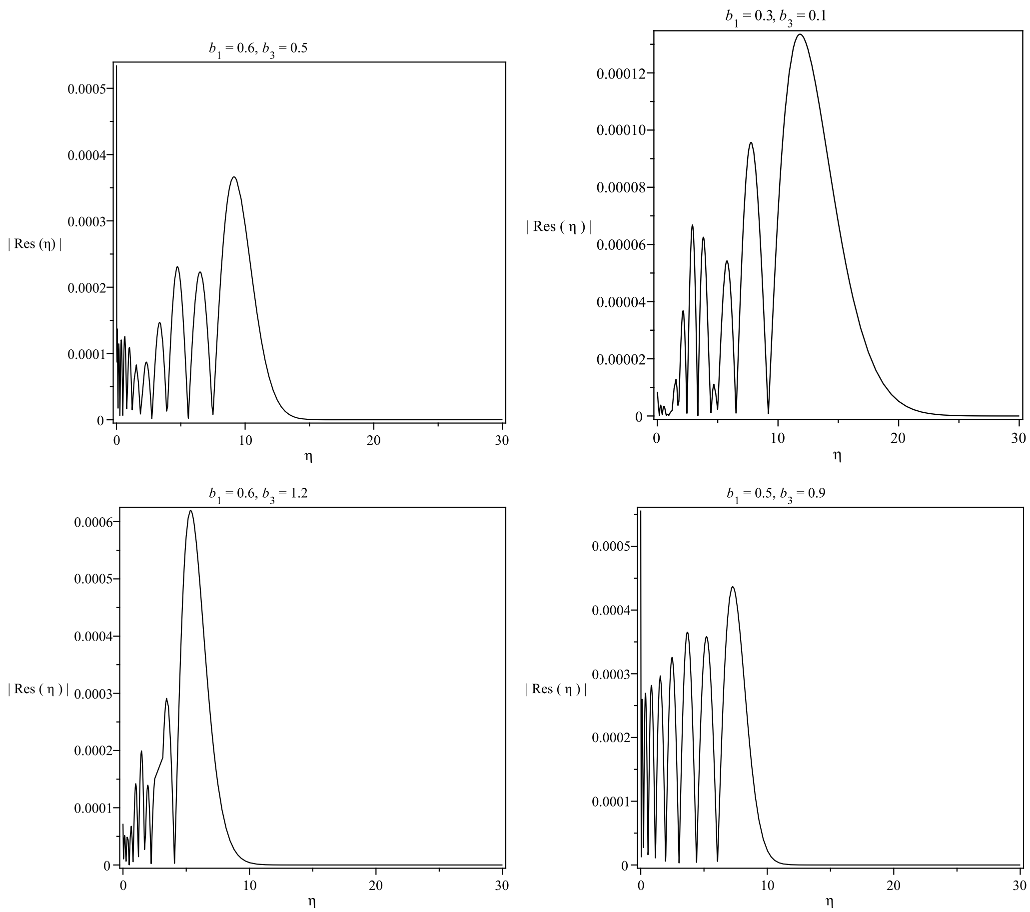

neural network had reduced the computational time which makes this method better than the conventional methods. The proposed solver have some advantages over other numerical techniques: solutions are readily available on any continuous input within the entire trained interval, whereas other numerical solvers give results only on a predefined grid with discrete inputs. Also analytical solvers like ADM, VIM, HPM and HAM give accurate results only in a close vicinity of the initial guess; as the input range expands, they start to accumulate error. The proposed neural network models on the other hand are less prone to these effects. Simplicity of concept, ease of implementation, and broader applicability domains are other perks of the proposed scheme.

Acknowledgment

The authors thank the associate editor and the referees for the accurate reading of the manuscript and the useful suggestions.

References

[1] S. Abbasbandy, T. Hayat, H.R. Ghehsareh, A Alsaedi, *MHD Falkner-Skan flow of Maxwell fluid by rational Chebyshev collocation method*, Applied Mathematics and Mechanics, *34(8)* (2013), 921–930.

[2] S. Abbasbandy, H. Roohani Ghehsareh, *Solutions for MHD viscous flow due to a shrinking sheet by Hankel-Pade method*, International Journal of Numerical Methods for Heat Fluid Flow, *23(2)* (2013), 388–400.

[3] S. Abbasbandy, H. Roohani Ghehsareh, *Solutions of the magnetohydrodynamic flow over a nonlinear stretching sheet and nano boundary layers over stretching surfaces*, International Journal for Numerical Methods in Fluids, *70* (2012), 1324–1340.

[4] S. Abbasbandy, H. Roohani Ghehsareh, I. Hashim, *An accurate solution for the steady flow of third-grade fluid in a porous half space*, Walailak. J. Sci. Tech., *9(2)* (2012),153–163.

[5] S. Abbasbandy, H. Roohani Ghehsareh, I. Hashim, *An approximate solution of the MHD flow over a non-linear stretching sheet by rational Chebyshev collocation method*, UPB Sci. Bull., *74(4)* (2012), 1223–7027.

[6] F. Ahmad, *A simple analytical solution for the steady flow of a third grade fluid in a porous half space*, Commun. Nonlinear. Sci. Numer. Simulat., *14* (2009), 2848-2852.

[7] F. Baharifard, S. Kazem, K Parand, *Rational and Exponential Legendre Tau Method on Steady Flow of a Third Grade Fluid in a Porous Half Space*, International Journal of Applied and Computational Mathematics, *2(4)* (2016), 679–698.

[8] R.S. Beidokhti, A. Malek, *Solving initial-boundary value problems for systems of partial differential equations using neural networks and optimization techniques*, Journal of The Frankl in Institute, *346(9)* (2009), 898–913.

[9] M.D. Buhmann, *Radial Basis Functions: Theory and Implementations*, Cambridge University Press, New York, 2004.

[10] N. Duvvuru, K.S. Swarup, *Ahybrid interior point assisted differential evolution algorithm for economic dispatch*, IEEE Trans. Power Systems, *26(2)* (2011), 541–549.

[11] G.E. Fasshauer, *Meshfree Approximation Methods with MATLAB*, World Scientific Publishing Co. Pte. Ltd. Uchaikin, 2007.

[12] T. Hayat, F. Shahzad, M. Ayub, *Analytical solution for the steady flow of the third grade fluid in a porous half space*, Appl. Math. Model., *31* (2007), 2424–2432.

[13] T. Hayat, F. Shahzad, M. Ayub, S. Asghar, *Stokes first problem for a third grade fluid in a porous half space*, Commun. Nonlin. Sci. Numer. Simul., *13* (2008), 1801–1807.

[14] D.R. Parisi, M.C. Mariani, M.A. Laborde, *Solving differential equations with unsupervised neural networks*, Chemical Engineering and Processing, *42(8-9)* (2003), 715–721.

[15] M. Powell, *The Theory of Radial Basis Function Approximation in 1990*, Oxford, Clarendon, 1992.

[16] K.R. Rajagopal, A.S. Gupta, *An exact solution for the flow of a non-Newtonian fluid past an infinite porous plate*, Meccanica, *19(2)* (1984), 158–160.

[17] K.R. Rajagopal, T.Y. Na, *On Stokes' problem for a non-Newtonian fluid*, Acta Mechanica, *48(3-4)* (1983), 233–239.

[18] H. Roohani Ghehsareh, S. Abbasbandy, M.A. Kutbi, A. Zaghian. *A Comparative Study Between two Explicit and Minimal Strategies for the Case of Magnetohydrodynamical Falkner-Skan Flow over a Permeable Wall*, Zeitschrift fr Naturforschung A, *69(a)* (2014), 263–272.

[19] H. Roohani Ghehsareh, K. Karimi, A. Zaghian, *Numerical solutions of a mathematical model of blood flow in the deforming porous channel using radial basis function collocation method*, Journal of the Brazilian Society of Mechanical Sciences and Engineering, *38(3)* (2016), 709–720.

[20] W. Tan, T. Masuoka, *Stokes first problem for a second grade fluid in a porous half space with heated boundary*, Int. J. Non-Linear Mech., *40* (2005), 515–522.

[21] C. Wen, Z.J. Fu, C.S. Chen, *Recent Advances in Radial Basis Function Collocation Method*, Heidelberg: Springer, 2014.

[22] M.H. Wright, *The interior-point revolution in optimization: history, recent developments, and lasting consequences*, Bulletin of the American Mathemattical Society (N.S), *42* (2005), 39–56.

[23] W. Yan, L. Wen, W. Li, C.Y. Chung, K.P. Wong, *Decomposition-coordination interior point method and its application to multi-area optimal reactive power flow*, International Journal of Electrical Power Energy Systems, *33(1)* (2011), 55–60.